# Incorporation of charge- and pair-density-wave states into the one-band model of *d*-wave superconductivity

Michał Zegrodnik[1,*] and Józef Spałek[2,†]

[1]*Academic Centre for Materials and Nanotechnology, AGH University of Science and Technology, Aleja Mickiewicza 30, 30-059 Kraków, Poland*

[2]*Marian Smoluchowski Institute of Physics, Jagiellonian University, ulica Łojasiewicza 11, 30-348 Kraków, Poland*

(Received 1 September 2018; published 29 October 2018)

We study the coexistence of pair- (PDW) and charge-density-wave (CDW) states within the single-band $t$-$J$-$U$ and Hubbard models of $d$-wave superconductivity and discuss our results in the context of the experimental observations for the copper-based compounds. In order to take the correlation effects into account with proper precision, we use the approach based on the diagrammatic expansion of the Gutzwiller wave function (DE-GWF), which goes beyond the renormalized mean-field theory in a systematic manner. According to our analysis of the $t$-$J$-$U$ model, the transition between the pure $d$-wave superconducting phase and the coexistent CDW+PDW phase takes place at $\delta \approx 0.18$ (close to the optimal doping), with the modulated phase located in the underdoped regime. The situation is different for the case of the Hubbard model, where a narrow stability regime of a precursor nematic phase sets in preceding the formation of the modulated CDW+PDW state, with decreasing hole doping. The results conclude our comprehensive discussion of the standard phase diagram for high-$T_C$ superconducting compounds within the DE-GWF variational approach in the single narrow-band case [see J. Spałek *et al.*, Phys. Rev. B **95**, 024506 (2017); M. Zegrodnik and Spałek, *ibid.* **95**, 024507 (2017); **96**, 054511 (2017); New J. Phys. **20**, 063015 (2018)].

DOI: 10.1103/PhysRevB.98.155144

## I. INTRODUCTION

The charge-density-wave (CDW) state plays an important role in the physics of underdoped copper-based high-$T_C$ superconducting (SC) compounds. For yttrium- (yttrium barium copper oxide, YBCO) and Bi- and Hg-based materials, the incommensurate CDW modulation vectors $\mathbf{Q}$ lie in the copper oxide plane and have the forms $(0, Q)2\pi/a$ and $(Q, 0)2\pi/a$ ($a$ is the Cu-O lattice constant) [1–5], with a weakly doping dependent periodicity $Q \approx 0.25$–$0.3$ [2,3,5–8]. It is still under debate whether the proximity of the vector $\mathbf{Q}$ to the vectors connecting neighboring hot spots at the Fermi surface is only a coincidence or, in fact, the Fermi surface topology imposes the CDW periodicity. Both the charge stripes with 90° rotated domains and the checkerboard pattern are consistent with the two simultaneously measured modulation vectors, and it is not settled as yet which scenario is realized experimentally. Nevertheless, some reports point to the charge stripes as the actual form of the CDW state [9].

For the La-based cuprates, in which the charge order was initially observed, it has been confirmed that uniaxial stripe domains with a periodicity of $\sim 4a$ are formed [10–12]. However, in this case an arrangement of combined charge and spin order is believed to appear simultaneously. Also, other significant differences between the majority of the cuprate family and the La-based cuprates appear when it comes to the discussion of the charge-ordered phase [9,13,14]. In our considerations we refer mainly to the former systems.

Since both the high-temperature superconductivity and CDW phase appear in the same doping range of the phase diagram (the underdoped regime), a natural question concerns the interplay between the two phases. The experimental data clearly show the competition between the CDW and SC, which is manifested by the plateau in the SC critical temperature in the underdoped regime, as well as by the suppression of the CDW intensity peak and correlation length below $T_C$ [3–5,15,16]. Another issue which concerns the relationship between the two phases is the possibility of spatially modulated Cooper-pair density, which could coexist with charge ordering in the underdoped regime. Such a pair-density-wave (PDW) state has some principal similarities to the Fulde-Ferrell-Larkin-Ovchinnikov state, which has been proposed in various systems [17–21]. Very recently, the PDW state was reported experimentally in $Bi_2Sr_2CaCu_2O_{8+x}$ (BSCCO) [22], and it was found that the pair-density and charge-density modulations are governed by very similar vectors, $\mathbf{Q} \approx (0.25, 0)2\pi/a$ and $\mathbf{Q} \approx (0, 0.25)2\pi/a$. Such an observation is consistent with the Ginzburg-Landau theory of a $d$-wave superconductor coexisting with the $d$-symmetry form factor charge density wave [23–25]. The coexistent CDW+PDW state with $Q_{CDW} = Q_{PDW}$ has also been studied theoretically within the microscopic spin-fermion and Hubbard models [25–27]. In the latter case, the variational cluster approximation has been used, and the stability of the PDW+CDW state has been shown to appear at $\delta > 0.08$ (the calculations were carried out only for $\delta < 0.15$; see Fig. 7 in Ref. [26]). For the case of the spin-fermion model [25] it was argued

*michal.zegrodnik@agh.edu.pl
†jozef.spalek@uj.edu.pl

 

that the PDW+CDW phase should appear in the underdoped regime with a pure $d$-wave superconducting phase appearing above the optimal doping, which is in accordance with the experimental expectations. One should also note the recent experimental and theoretical results concerning the appearance of the PDW and CDW coexistence within the vortex core halo, which, however, do not correspond directly to the situation presented here [28–33].

Here, we analyze theoretically the PDW and CDW coexistence within the single-band Hubbard and $t$-$J$-$U$ models with the inclusion of correlation effects by going beyond the renormalized mean-field theory (RMFT) approach in a systematic manner. Namely, we use the *diagrammatic expansion of the Gutzwiller wave function* (DE-GWF) method, which allows us to obtain the full Gutzwiller wave function solution for the modulated states and to study their stability as a function of doping. It was shown previously that by accounting for the electron correlations already at the level of RMFT one can obtain the proper charge-ordering modulations with a dominant $d$-form factor within the $t$-$J$-$V$ model [34]. In these considerations the intersite Coulomb interaction term ($\sim V$) is necessary to induce the charge-ordered phase. However, a similar result can also be obtained within alternative approaches [35–38].

As we show below, by using the DE-GWF method, the CDW modulation appears already within the Hubbard model (with only intrasite repulsion), which is one of the canonical one-band models used for the description of the Cu-O planes in copper-based materials. Furthermore, we also study the $t$-$J$-$U$ model, for which we recently obtained very good quantitative agreement between theory and experiment for the selected principal observations of the $d$-wave superconducting state in cuprates (the motivation for using such an extended model is discussed in Ref. [39]). With this analysis, we extend our previous considerations of pure $d$-wave superconductivity to the description of both charge- and Cooper-pair-modulated states. Within our study both the PDW and CDW states are modulated according to a fixed single commensurate vector $\mathbf{Q} = (1/3, 0)2\pi/a$, which is close to the incommensurate one measured in experiment [4,7,9]. Such an approach is justified by the very weak measured doping dependence of $\mathbf{Q}$ [5] and the close proximity of the PDW and CDW modulation vectors reported in experiments [22]. In our calculations we allow for both the site-centered ($s$-wave) and bond-centered ($d$-wave, extended $s$-wave) CDWs. The former corresponds to a situation in which the on-site electron concentration is modulated, whereas for the latter the electron hopping value is modulated.

We show that for the model with both a small but nonzero number of double occupancies and the intersite exchange interaction term included explicitly ($t$-$J$-$U$ model), the stability of the coexistent PDW+CDW modulated state is contained in the underdoped regime, and the pure $d$-wave SC phase occurs at and above the optimal doping on the phase diagram and thus reproduces the experimental situation. However, the issue of the modulation form factor still seems to remain problematic since in our analysis the site-centered CDW contribution appears to be significant, in contradiction to the experimental data, where the nodal, $d$-wave-type modulation persists to the lowest possible doping in the metallic phase.

The structure of the paper is as follows. In the next section we present the theoretical model and its solution. Section III contains detailed numerical results and a discussion of them. The conclusions are contained in the last section.

## II. THEORY

### A. Model and wave function

The Hamiltonian considered here is [39–42]

$$\hat{\mathcal{H}} = t\sum_{\langle ij\rangle\sigma}\hat{c}^{\dagger}_{i\sigma}\hat{c}_{j\sigma} + t'\sum_{\langle\langle ij\rangle\rangle\sigma}\hat{c}^{\dagger}_{i\sigma}\hat{c}_{j\sigma} + J\sum_{\langle ij\rangle}\hat{\mathbf{S}}_i\cdot\hat{\mathbf{S}}_j + U\sum_i \hat{n}_{i\uparrow}\hat{n}_{i\downarrow}, \tag{1}$$

where the first two terms correspond to the single-electron hoppings, the third represents the antiferromagnetic superexchange interaction, and the last refers to the intrasite Coulomb repulsion. By $\langle\cdots\rangle$ and $\langle\langle\cdots\rangle\rangle$ we denote the summations over the nearest neighbors and next-nearest neighbors, respectively. For $J \equiv 0$ we obtain the Hubbard model which is also considered here, whereas for the case of $U \to \infty$ (i.e., $U \gg |t|$) we reproduce the $t$-$J$ model. Formally, this model describes an interpolation between the Hubbard and $t$-$J$ model limits. Physically, it extends the concept of kinetic exchange to the situation when $U$ is not too large compared to the bare bandwidth $W$.

This extended model was discussed in detail by us previously and applied to a quantitative analysis of selected universal properties of cuprate high-$T_C$ superconductors within our original diagrammatic solution of the Gutzwiller wave function in two dimensions [39–41]. Also, the effect of nematicity on the resulting phase diagram was discussed by us recently [42]. In what follows we supplement our extensive analysis by incorporating the CDW/PDW solution into the scheme.

In order to take into account interelectronic correlations we use the DE-GWF approach to the Gutzwiller-type wave function defined by

$$|\Psi_G\rangle \equiv \hat{P}_G|\Psi_0\rangle, \tag{2}$$

where $|\Psi_0\rangle$ is the noncorrelated wave function (which will be defined later) and the correlation operator $\hat{P}_G$ is

$$\hat{P}_G \equiv \prod_i \hat{P}_i = \prod_i \sum_{\Gamma} \lambda_{i,\Gamma}|\Gamma\rangle_{ii}\langle\Gamma|, \tag{3}$$

where $\lambda_{i,\Gamma} \in \{\lambda_{i\emptyset}, \lambda_{i\uparrow}, \lambda_{i\downarrow}, \lambda_{id}\}$ are the variational parameters which correspond to four states from the local basis $|\emptyset\rangle_i$ , $|\uparrow\rangle_i$ , $|\downarrow\rangle_i$ , $|\uparrow\downarrow\rangle_i$ at site $i$, respectively.

An important step of the DE-GWF method is the application of the condition [43,44]

$$\hat{P}_i^2 \equiv 1 + x_i\hat{d}_i^{\mathrm{HF}}, \tag{4}$$

where $x_i$ is yet another variational parameter and $\hat{d}_i^{\mathrm{HF}} \equiv \hat{n}_{i\uparrow}^{\mathrm{HF}}\hat{n}_{i\downarrow}^{\mathrm{HF}}$, $\hat{n}_{i\sigma}^{\mathrm{HF}} \equiv \hat{n}_{i\sigma} - n_{i\sigma}^{(0)}$, with $n_{i\sigma}^{(0)} \equiv \langle\Psi_0|\hat{n}_{i\sigma}|\Psi_0\rangle$. One should note that $\lambda_{i,\Gamma}$ parameters for a given site $i$ are functions of $x_i$, which means that there is a single variational parameter per atomic site in such an approach. As has been shown in Refs. [43,44], condition (4) leads to the rapid convergence of the resulting diagrammatic expansion with the increasing

order of the variational parameter $x_i$. For the case of a spatially homogeneous state one has $x_i \equiv x$. The formulation and discussion of the DE-GWF approach for the case of homogeneous $d$-wave superconducting or paramagnetic states are provided in Refs. [43–46]. For the case of the CDW/PDW states the $x_i$ parameter follows the modulation which characterizes those new ordered phases. In what follows we denote the normalized expectation values in the correlated state by $\langle\cdots\rangle_G = \langle\Psi_G|\cdots|\Psi_G\rangle/\langle\Psi_G|\Psi_G\rangle$, while the corresponding expectation values in the noncorrelated state are denoted $\langle\cdots\rangle_0 = \langle\Psi_0|\cdots|\Psi_0\rangle$.

### B. CDW and PDW states: A general characterization

In order to encompass both site- and bond-centered charge orderings, as well as the PDW phase appearance, one has to allow for a modulation of the hopping averages $\langle\hat{c}^\dagger_{i\sigma}\hat{c}_{j\sigma}\rangle_G$, electron concentration $\langle\hat{n}_i\rangle_G$, and pairing averages $\langle\hat{c}^\dagger_{i\uparrow}\hat{c}^\dagger_{j\downarrow}\rangle_G$ in the considered wave function. Assuming that all three types of averages are modulated by a single vector, one can write

$$\langle\hat{c}^\dagger_{i\sigma}\hat{c}_{j\sigma}\rangle_G = \bar{P}_{\mathbf{g}_{ij}} + \delta P_{\mathbf{g}_{ij}}\cos[\mathbf{Q}(\mathbf{R}_j + \mathbf{g}_{ij}/2)], \tag{5}$$

$$\langle\hat{n}_{i\sigma}\rangle_G = \bar{n} + \delta n_{CDW}\cos[\mathbf{Q}\mathbf{R}_i], \tag{6}$$

$$\langle\hat{c}^\dagger_{i\uparrow}\hat{c}^\dagger_{j\downarrow}\rangle_G = \bar{\Delta}_{\mathbf{g}_{ij}} + \delta\Delta_{\mathbf{g}_{ij}}\cos[\mathbf{Q}(\mathbf{R}_j + \mathbf{g}_{ij}/2)], \tag{7}$$

where $\mathbf{g}_{ij} = \mathbf{R}_i - \mathbf{R}_j$ and $\mathbf{Q}$ is the modulation vector. Note that the reference values $\bar{P}_{\mathbf{g}_{ij}}$ and $\bar{\Delta}_{\mathbf{g}_{ij}}$ and the modulation amplitudes $\delta P_{\mathbf{g}_{ij}}$ and $\delta\Delta_{\mathbf{g}_{ij}}$ depend only on the vector connecting sites $i$ and $j$. Equations (5) and (7) correspond to only $i \neq j$ since we do not include the intrasite pairing in our approach. As one can realize, in that situation the DE-GWF solution will contain a number of self-consistent integral equations, and thus, the computations are quite involved.

As already stated in the preceding section, here, we represent the modulation by a single commensurate vector in the form $\mathbf{Q} = (1/3, 0)2\pi/a$, which is close to the incommensurate one measured in experiments [4,7,9]. Such a choice leads to a modulation along the $x$ axis with a period of $3a$ in real space. A schematic illustration of how the electron concentration and hopping averages change in real space is provided in Fig. 1. As we can see, there is a repeating pattern of three consecutive atomic sites labeled by (0), (1), and (2) [see Fig. 1(b)]. Atomic sites (1) and (2) have the same value of $\langle\hat{n}_{i\sigma}\rangle$, which differs from that on site (0). An analogous repeating pattern can be found for the hopping averages (marked by the solid and dashed lines) and the pairing averages (not shown for the sake of clarity).

In our diagrammatic approach we assume that the hopping and pairing averages in the noncorrelated ($|\Psi_0\rangle$) and correlated ($|\Psi_G\rangle$) states can have nonzero values up to the fourth-nearest neighbor. This represents the real-space cutoff, which will be discussed briefly in the next section when the diagrammatic method is described. All the nonzero averages taken into account are modulated according to Eqs. (5)–(7). However, the dominant contribution to the wave function comes from the nearest- and next-nearest-neighbor expectation values. Therefore, for the sake of clarity we focus here on the analysis of the modulations of the on-site electron

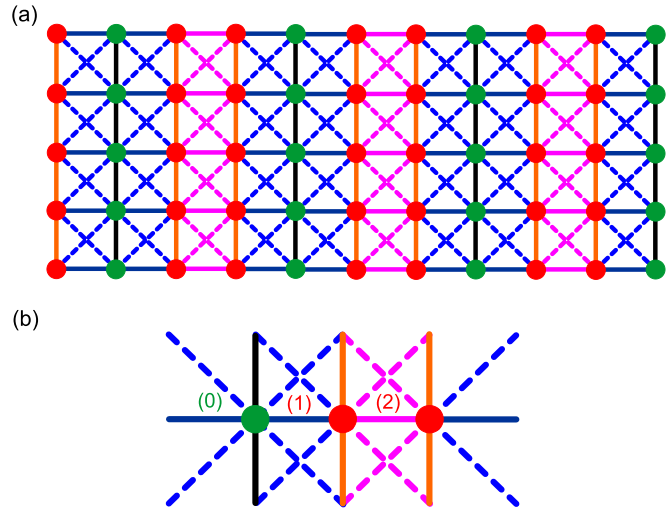


FIG. 1. (a) Schematic illustration of charge modulation on a square lattice with the vector $\mathbf{Q} = (1/3, 0)2\pi/a$. Dots and lines with different colors correspond to different values of $\langle\hat{n}_{i\sigma}\rangle$ and $\langle\hat{c}^\dagger_{i\sigma}\hat{c}_{j\sigma}\rangle$ averages, respectively. The nearest-neighbor hopping averages are marked by the solid lines, while the next-nearest-neighbor averages are marked by the dashed lines. (b) The three atomic sites which compose the repeating pattern and are enumerated by (0), (1), and (2). Concentrations on sites (1) and (2) are equal and different from that on site (0).

concentration $\langle\hat{n}_{i\sigma}\rangle_G$, the nearest- and next-nearest-neighbor hopping averages $\langle\hat{c}^\dagger_{i\sigma}\hat{c}_{j\sigma}\rangle_G$, and the nearest-neighbor pairing averages $\langle\hat{c}^\dagger_{i\uparrow}\hat{c}^\dagger_{j\downarrow}\rangle_G$ (since the diagonal next-nearest-neighbor pairing contribution is zero due to the $d$-wave symmetry of the pairing).

For the selected modulation vector it is convenient to use the following site-dependent hopping and pairing parameters representing the considered symmetries:

$$\begin{aligned} P_i^{d,s',x} &= \frac{1}{4}\sum_{\langle j(i)\rangle}\gamma_{ij}^{d,s',x}\langle\hat{c}^\dagger_{j\sigma}\hat{c}_{i\sigma}\rangle_G, \\ P_i^{s'',x'} &= \frac{1}{4}\sum_{\langle\langle j(i)\rangle\rangle}\gamma_{ij}^{s'',x'}\langle\hat{c}^\dagger_{j\sigma}\hat{c}_{i\sigma}\rangle_G, \\ \Delta_i^{d,s',x} &= \frac{1}{4}\sum_{\langle j(i)\rangle}\gamma_{ij}^{d,s,x}\langle\hat{c}^\dagger_{j\uparrow}\hat{c}^\dagger_{i\downarrow}\rangle_G, \end{aligned} \tag{8}$$

where $\langle j(i)\rangle$ [$\langle\langle j(i)\rangle\rangle$] denotes the summation over the nearest (next-nearest) neighbors of atomic site $i$. The symmetry factors are defined as

$$\begin{aligned} \gamma_{ij}^{d} &= (\delta_{\mathbf{g}_{ij}-\hat{x}} + \delta_{\mathbf{g}_{ij}+\hat{x}} - \delta_{\mathbf{g}_{ij}-\hat{y}} - \delta_{\mathbf{g}_{ij}+\hat{y}}), \\ \gamma_{ij}^{s'} &= (\delta_{\mathbf{g}_{ij}-\hat{x}} + \delta_{\mathbf{g}_{ij}+\hat{x}} + \delta_{\mathbf{g}_{ij}-\hat{y}} + \delta_{\mathbf{g}_{ij}+\hat{y}}), \\ \gamma_{ij}^{x} &= (\delta_{\mathbf{g}_{ij}-\hat{x}} - \delta_{\mathbf{g}_{ij}+\hat{x}}), \\ \gamma_{ij}^{s''} &= (\delta_{\mathbf{g}_{ij}-\hat{x}-\hat{y}} + \delta_{\mathbf{g}_{ij}+\hat{x}+\hat{y}} + \delta_{\mathbf{g}_{ij}+\hat{x}-\hat{y}} + \delta_{\mathbf{g}_{ij}+\hat{x}+\hat{y}}), \\ \gamma_{ij}^{x'} &= (\delta_{\mathbf{g}_{ij}-\hat{x}-\hat{y}} - \delta_{\mathbf{g}_{ij}+\hat{x}+\hat{y}} - \delta_{\mathbf{g}_{ij}+\hat{x}-\hat{y}} + \delta_{\mathbf{g}_{ij}-\hat{x}+\hat{y}}), \end{aligned} \tag{9}$$

with $\delta_{\mathbf{v}}$ being the appropriate Kronecker delta. The parameters $P_i^d$ ($\Delta_i^d$), $P_i^{s'}$ ($\Delta_i^{s'}$), and $P_i^{s''}$ correspond to the $d$-wave and extended $s$-wave hopping (pairing) contributions to the wave

function, respectively. Note also that the nonzero values of both $P_i^d$ ($\Delta_i^d$) and $P_i^{s'}$ ($\Delta_i^{s'}$) lead to breaking of the $C_4$ symmetry, which still does not imply the presence of charge ordering, as such a condition can be fulfilled also in the homogeneous nematic (coexistent nematic-superconducting) state. The CDW (PDW) phase appears only when $P_i^{d,s',s''}$ ($\Delta_i^{d,s'}$) becomes site dependent according to the modulation $\mathbf{Q}$. In such a situation the hopping (pairing) averages from atomic sites (1) and (2) to the left-hand neighbor can be different from the corresponding right-hand hopping (pairing), which leads to nonzero values of $P_i^x$ ($\Delta_i^x$; see Fig. 1). The latter rule also applies to the next-nearest neighbors, which results in nonzero values of $P_i^{x'}$. The pairing parameters analogical to $P_i^{s''}$ and $P_i^{x'}$ do not appear since the pairing in the diagonal direction is zero.

Using Eqs. (5)–(8), we can write

$$P_i^{d,s',s''} = \bar{P}^{d,s',s''} + \delta P_{CDW}^{d,s',s''} \cos[\mathbf{Q}\mathbf{R}_i], \tag{10}$$

$$\Delta_i^{d,s'} = \bar{\Delta}^{d,s'} + \delta \Delta_{PDW}^{d,s'} \cos[\mathbf{Q}\mathbf{R}_i], \tag{11}$$

$$P_i^{x,x'} = \delta P_{CDW}^{x,x'} \sin[\mathbf{Q}\mathbf{R}_i], \tag{12}$$

$$\Delta_i^{x} = \delta \Delta_{PDW}^{x} \sin[\mathbf{Q}\mathbf{R}_i], \tag{13}$$

where $\bar{P}^{d,s',s''}$ and $\bar{\Delta}^{d,s'}$ are the site-independent reference values and $\delta P_{CDW}^{d,s',s'',x,x'}$ and $\delta \Delta_{PDW}^{d,s',x}$ are the symmetry-resolved modulation amplitudes. The amplitudes appearing in Eqs. (5) and (7) can be expressed by $\delta P_{CDW}^{d,s',s'',x,x'}$ and $\delta \Delta_{PDW}^{d,s',x}$ in the following manner:

$$\begin{aligned}\delta P_{\mathbf{g}_{ij}} = {} & \delta P_{CDW}^{d} \, \gamma_{ij}^{d} + \delta P_{CDW}^{s'} \, \gamma_{ij}^{s'} + 2\delta P_{CDW}^{x} \, \gamma_{ij}^{x} \\ & + \delta P_{CDW}^{s''} \, \gamma_{ij}^{s''} + \delta P_{CDW}^{x'} \, \gamma_{ij}^{x'},\end{aligned} \tag{14}$$

$$\delta \Delta_{\mathbf{g}_{ij}} = \delta \Delta_{PDW}^{d} \, \gamma_{ij}^{d} + \delta \Delta_{PDW}^{s'} \, \gamma_{ij}^{s'} + 2\delta \Delta_{PDW}^{x} \, \gamma_{ij}^{x}, \tag{15}$$

from which we can see the resulting modulation can be expressed as a mixture of the considered symmetry contributions. The same applies to the reference values $\bar{P}_{CDW}^{d,s',s'',x,x'}$ and $\bar{\Delta}_{PDW}^{d,s',x}$.

The nonzero value of $\delta P_{CDW}^{d,s',s'',x,x''}$ in Eq. (14) corresponds to the bond-centered CDW, while the nonzero value of $\delta n_{CDW}$ in Eq. (6) is responsible for the site-centered CDW. The remaining modulation amplitudes $\delta \Delta_{PDW}^{d,s',x}$ in Eq. (15) introduce the PDW phase. All those modulation amplitudes play the role of order-parameter components of the CDW and/or PDW states.

### C. Solution methodology

For the correlated wave function $|\Psi_G\rangle$ with the selected modulation, the expectation value from any two local operators, $\hat{o}_i$ and $\hat{o}'_j$ appearing in the initial Hamiltonian (1), can be expressed in the form (cf. Refs. [40,45])

$$\langle \Psi_G | \hat{o}_i \hat{o}'_j | \Psi_G \rangle = \sum_{k=0}^{\infty} \frac{1}{k!} {\sum_{l_1 \cdots l_k}}' x_0^{k_0} x_1^{k_1} x_2^{k_2} \langle \Psi_0 | \tilde{o}_i \tilde{o}'_j \, \hat{d}^{\mathrm{HF}}_{l_1 \cdots l_k} | \Psi_0 \rangle, \tag{16}$$

where $\tilde{o}_i \equiv \hat{P}_i \hat{o}_i \hat{P}_i$, $\tilde{o}'_j \equiv \hat{P}_j \hat{o}'_j \hat{P}_j$, $\hat{d}^{\mathrm{HF}}_{l_1 \cdots l_k} \equiv \hat{d}^{\mathrm{HF}}_{l_1} \cdots \hat{d}^{\mathrm{HF}}_{l_k}$, and $\hat{d}^{\mathrm{HF}}_{\varnothing} \equiv 1$. The primed summation has the following restrictions: $l_p \neq l_{p'}$, $l_p \neq i, j$ for all $p$ and $p'$. The variational parameters $x_0$, $x_1$, and $x_2$ correspond to the three atomic positions from the repeating pattern depicted in Fig. 1. Since atomic sites (1) and (2) are equivalent, one can take $x_1 \equiv x_2$. For a given term of the summation over $l_1 \cdots l_k$, the powers $k_0$, $k_1$, and $k_2$ represent how many times in the set $l_1 \cdots l_k$ the indices corresponding to (0), (1), and (2) appear, respectively. They fulfill the relation $k_0 + k_1 + k_2 = k$. It has been shown [45,47] that the desired convergence can be achieved by taking the first four to six terms of the summation over $k$ appearing in Eq. (16). The results presented in the subsequent section were obtained by including terms up to third order in $k$.

The averages in the noncorrelated state $|\Psi\rangle_0$ on the right-hand side of Eq. (16) can be decomposed with the use of Wick's theorem and expressed in terms of the correlation functions $P_{ij\sigma}^{(0)} \equiv \langle \hat{c}_{i\sigma}^{\dagger} \hat{c}_{j\sigma} \rangle_0$ and $\Delta_{ij}^{(0)} \equiv \langle \hat{c}_{i\uparrow}^{\dagger} \hat{c}_{j\downarrow}^{\dagger} \rangle_0$. Such a procedure allows us to express the ground-state energy $\langle \hat{\mathcal{H}} \rangle_G \equiv \langle \Psi_G | \hat{\mathcal{H}} | \Psi_G \rangle / \langle \Psi_G | \Psi_G \rangle$ as a function of $P_{ij\sigma}^{(0)}$, $\Delta_{ij}^{(0)}$, $n_{i\sigma}^{(0)}$, and $x_m$. In practice, it is necessary to introduce the real-space cutoff for the $P_{ij\sigma}^{(0)}$ and $\Delta_{ij}^{(0)}$ parameters. Here, in order to carry out the calculations in a reasonable time, the maximum distance has been taken to be $R_{\max}^2 = 5a^2$, which means that we include the hopping and pairing averages up to the fourth nearest neighbor.

Having an explicit formula for the energy expectation values in different phases, one can derive the effective Schrödinger equation and the set of self-consistent equations for the parameters $P_{ij\sigma}^{(0)}$ and $\Delta_{ij}^{(0)}$, in a manner similar to that in Refs. [40,45]. The set of equations is solved in conjunction with the minimization of the energy with respect to $x_0$ and $x_1 \equiv x_2$. Having the values of $P_{ij\sigma}^{(0)}$, $\Delta_{ij}^{(0)}$, $x_0$, $x_1$, $x_2$, and $n_{i\sigma}^{(0)}$, one can calculate the correlated pairing averages $\langle \hat{c}_{i\uparrow}^{\dagger} \hat{c}_{j\downarrow}^{\dagger} \rangle_G$ and the correlated hopping averages $\langle \hat{c}_{i\sigma}^{\dagger} \hat{c}_{j\sigma} \rangle_G$. The latter values are, in turn, used to obtain the site-independent reference values $\bar{P}_{CDW}^{d,s,s',x,x'}$ and $\bar{\Delta}_{PDW}^{d,s,x}$ and the modulation amplitudes $\delta P_{CDW}^{d,s,s',x,x'}$, $\delta \Delta_{PDW}^{d,s,x}$, and $\delta n_{CDW}$ in the correlated state $|\Psi\rangle_G$.

One should note that when it comes to the modulated states, we assume that the hopping and pairing averages can be expressed by Eqs. (5) and (7) with $\mathbf{Q} = (1/3, 0)2\pi$ and that there is no spontaneous current created. Also, since the PDW phase emerges from the pure $d$-wave paired phase, we set the diagonal pairing averages to zero. We calculate all the listed symmetry factors with no further restrictions. Therefore, the relative balance between the particular symmetry contributions results explicitly from the calculations. The following phases appear to be stable within the analyzed approach and are discussed in the subsequent section:

For the paramagnetic phase (PM), $P_i^{s'} \equiv \bar{P}^{s'} \neq 0$, $P_i^{s''} \equiv \bar{P}^{s''} \neq 0$, $P_i^{d,x,x'} = 0$, $\Delta_i^{d,s',x} = 0$, $\delta P_{CDW}^{d,s',s'',x,x'} = \delta \Delta_{PDW}^{d,s',x} = 0$.

For the pure $d$-wave superconducting phase (SC), $P_i^{s'} \equiv \bar{P}^{s'} \neq 0$, $P_i^{s''} \equiv \bar{P}^{s''} \neq 0$, $\Delta_i^{d} \equiv \bar{\Delta}^{d} \neq 0$, $P_i^{d,x,x'} = 0$, $\Delta_i^{s',x} = 0$, $\delta P_{CDW}^{d,s',s'',x,x'} = \delta \Delta_{PDW}^{d,s',x} = 0$.

For the coexistent superconducting-nematic phase (SC+N), $P_i^{s'} \equiv \bar{P}^{s'} \neq 0$, $P_i^{s''} \equiv \bar{P}^{s''} \neq 0$, $P_i^{d} \equiv \bar{P}^{d} \neq 0$,

$\Delta_i^d \equiv \bar{\Delta}_d \neq 0$, $\Delta_i^{s'} \equiv \bar{\Delta}^{s'} \neq 0$, $P_i^{x,x'} \equiv 0$, $\Delta_i^x \equiv 0$, $\delta P_{CDW}^{d,s',x} = \delta \Delta_{PDW}^{d,s',x} \equiv 0$.

For the coexistent pair-density-wave and charge-density-wave phase (PDW+CDW), $\bar{P}^{d,s',s'',x,x'} \neq 0$, $\bar{\Delta}^{d,s',x} \neq 0$, $\delta P_{CDW}^{d,s',s'',x,x'} \neq 0$, $\delta \Delta_{PDW}^{d,s',x} \neq 0$.

## III. RESULTS AND DISCUSSION

First, we analyze the appearance of all the previously defined phases (PM, SC, SC+N, CDW+PDW) for the case of the Hubbard model, and subsequently, we discuss the effect of adding the exchange interaction term $\sim J$, which leads to the $t$-$J$-$U$ model. In that formulation the $t$-$J$ model is recovered as $U \to \infty$ ($U \gg t$) limit.

In Fig. 2 we display the correlated superconducting gaps (reference values $\bar{\Delta}$ and amplitudes $\delta\Delta_{PDW}$), correlated hoppings (reference values $\bar{P}$ and amplitudes $\delta P_{CDW}$), the amplitude of particle number modulations in real space $\delta n_{CDW}$, and the double occupancies, all as a function of hole doping for the case of the Hubbard model with $U = 18$ [$J \equiv 0$ in Hamiltonian (1)]. In the upper part of the figure we mark the stability regimes of particular phases. By going from the high-doping side we first encounter the PM phase with a vanishing superconducting gap, no charge ordering, and the $C_4$ symmetry conserved. For the dopings below $\delta \approx 0.35$ a pure $d$-wave SC phase is stable ($\bar{\Delta}^d \neq 0$). After passing the value $\delta \approx 0.28$, the $s$-wave component of the SC gap $\bar{\Delta}^s$ and the $d$-wave correlated hopping component $\bar{P}_d$ become nonzero, which signals the appearance of SC+N. An extensive analysis of the coexisting nematic-superconducting phase within the Hubbard and $t$-$J$-$U$ models is provided in Ref. [42]. The transition from the SC to SC+N phase is of second order. One can see that in the SC+N phase the $d$-wave component of the SC gap is reduced with respect to the case of the pure $d$-wave superconductivity, which is marked by the red dashed line in Fig. 2(a). In the nematic phase the $C_4$ symmetry is spontaneously broken, and the (1,0) and (0,1) directions are no longer equivalent in the electronic wave function, even though the underlying crystal lattice has no distortion (is still square). Moreover, in such a phase the translational symmetry is conserved, which means that no charge or SC gap modulation appears as yet ($\delta P_{CDW} = \delta n_{CDW} = \delta \Delta_{PDW} = 0$).

The SC+N phase can be understood to be a precursor of the PDW+CDW phase (for which the $C_4$ symmetry is also broken), which appears below the doping $\delta \approx 0.2$, at which a first-order transition takes place. In the PDW+CDW phase the SC gap, the average number of electrons, and the hopping averages are all modulated along the $x$ axis with the modulation vector $\mathbf{Q} = (1/3, 0)2\pi$. In this phase the pair-density wave coexists with both the site-centered and bond-centered charge orderings, and all the modulation amplitudes have nonzero values [$\delta P_{CDW} \neq 0$, $\delta n_{CDW} \neq 0$, $\delta \Delta_{PDW} \neq 0$; see Figs. 2(a), 2(b) and 2(c)]. For the sake of completeness, in Fig. 2(d) we plot the double occupancies corresponding to the three sublattices, which compose the pattern along the $x$ direction.

The results for the case of the $t$-$J$-$U$ model are presented in Fig. 3. As has already been reported in Ref. [42], the exchange term has a negative effect on the nematicity but a positive one on the superconductivity. The same can be seen here: for the $J$ value representative of cuprates ($J \approx 0.3$) the nematic phase is completely suppressed, while the stability of the superconducting phase is extended to higher doping values with respect to the Hubbard model case (see Fig. 2). As a result, the pure $d$-wave SC phase is stable down to the optimal doping value $\delta \approx 0.18$ at which a second-order phase transition appears to the PDW+CDW state without the

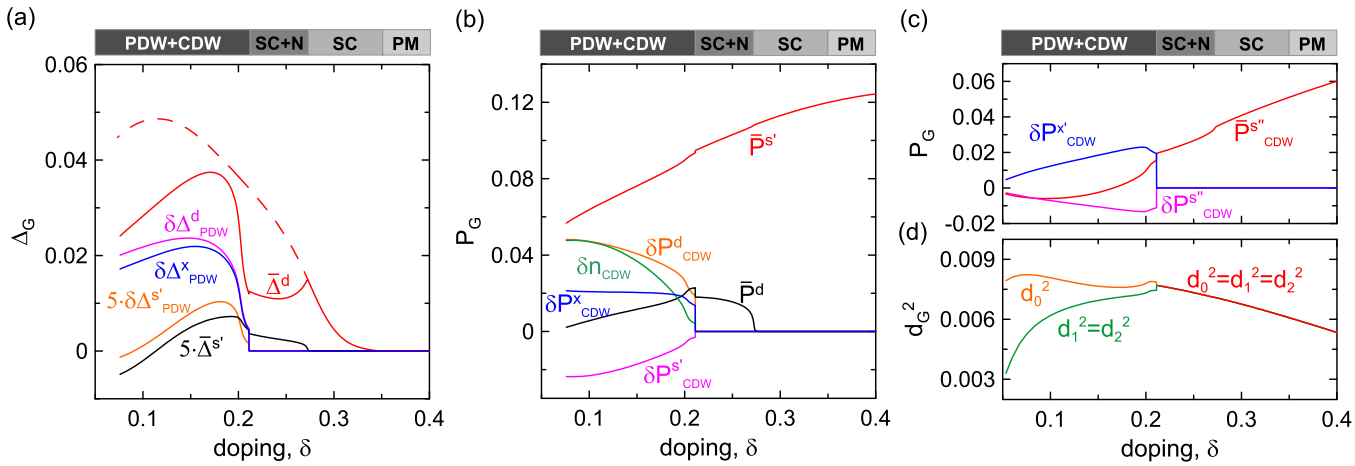


FIG. 2. Phase diagram for the case of the Hubbard model ($J \equiv 0$) for $U = 18$. (a) The $d$-wave and extended $s$-wave correlated gap reference values $\bar{\Delta}^d$ and $\bar{\Delta}^{s'}$, as well as the modulation amplitudes $\delta\Delta^d_{PDW}$, $\delta\Delta^{s'}_{PDW}$, and $\delta\Delta^x_{PDW}$ [see Eqs. (11) and (13)], all as functions of doping. Nonzero values of both $\bar{\Delta}^d$ and $\bar{\Delta}^{s'}$ signal the appearance of $C_4$ symmetry breaking, while $\delta\Delta_{PDW} \neq 0$ is evidence of SC gap modulation in real space, which in turn leads to the pair-density-wave state appearance. (b) and (c) Extended $s$-wave and $d$-wave hopping base values $\bar{P}^{s'}$, $\bar{P}^{s''}$ and $\bar{P}^d$, respectively, as well as the modulation amplitudes $\delta P^d_{CDW}$, $\delta P^{s'}_{CDW}$, $\delta P^{s''}_{CDW}$, $\delta P^x_{CDW}$, and $\delta P^{x'}_{CDW}$ [see Eqs. (10) and (12)] all as functions of doping. Nonzero values of both $\bar{P}^d$ and $\bar{P}^{s'}$ also signal the appearance of $C_4$ symmetry breaking, while $\delta P_{CDW} \neq 0$ is evidence of the average hopping modulations in real space, which in turn lead to the bond-centered charge-density-wave state. Additionally, for $\delta n_{CDW} \neq 0$ the site-centered charge-density-wave appears. (d) Double occupancies in the correlated state corresponding to the atomic sites labeled (0), (1), and (2) (see Fig. 1).

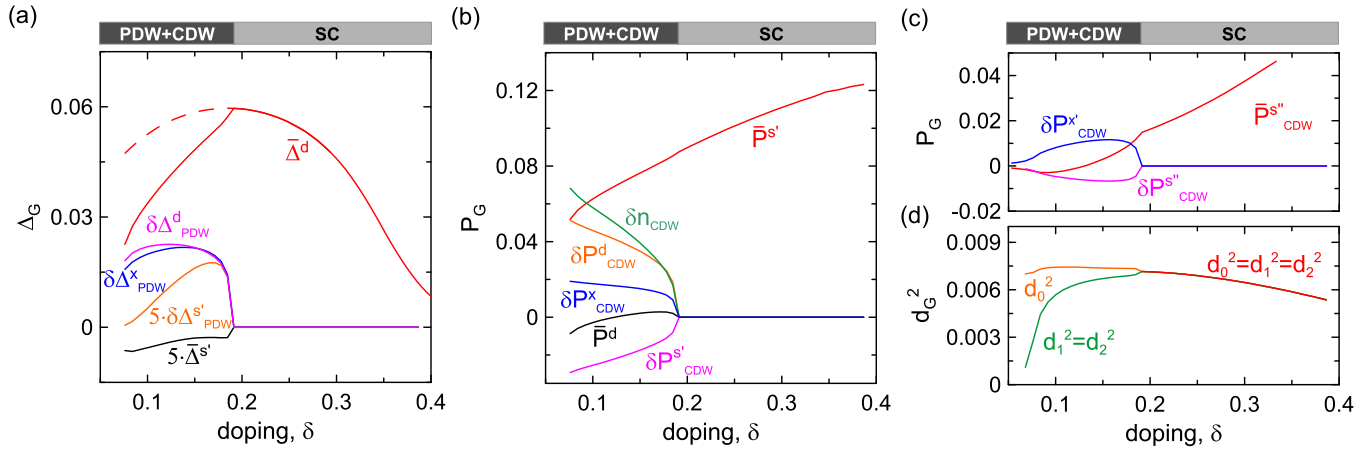


FIG. 3. Phase diagram for the case of the $t$-$J$-$U$ model with $J = 0.3$ and $U = 18$. (a) The $d$-wave and extended $s$-wave correlated gaps reference values $\bar{\Delta}^d$ and $\bar{\Delta}^{s'}$, as well as the modulation amplitudes $\delta\Delta^d_{PDW}$, $\delta\Delta^{s'}_{PDW}$, and $\delta\Delta^x_{PDW}$ [see Eqs. (11) and (13)], all as functions of doping. $\delta\Delta_{PDW} \neq 0$ is evidence of SC gap modulation in real space, which in turn leads to the pair-density-wave state appearance. (b) and (c) Extended $s$-wave and $d$-wave hopping reference values $\bar{P}^{s'}$, $\bar{P}^{s''}$ and $\bar{P}^d$, respectively, as well as the modulation amplitudes $\delta P^d_{CDW}$, $\delta P^{s'}_{CDW}$, $\delta P^{s''}_{CDW}$, $\delta P^x_{CDW}$, and $\delta P^{x'}_{CDW}$ [see Eqs. (10) and (12)] all as functions of doping. For dopings for which $\delta P_{CDW} \neq 0$ ($\delta n_{CDW} \neq 0$) the bond-centered (site-centered) charge-density-wave state sets in. (d) Double occupancies in the correlated state corresponding to the atomic sites labeled (0), (1), and (2) (see Fig. 1).

appearance of the precursor nematic phase in between the SC and PDW+CDW stability regimes. The red dashed line in Fig. 3(a) marks the continuation of the $d$-wave SC gap for the case when the PDW+CDW stability is not included in the calculations. In such a case the value $\delta \approx 0.18$ corresponds to the maximal correlated gap and hence the maximal critical temperature. The stability of the PDW+CDW phase in the underdoped regime obtained in our calculations reflects the experimental findings for the cuprates, where the charge-ordered phase is observed in a similar doping range [5,7,13]. The SC gap parameters' modulation amplitudes in the PDW+CDW phase are shown in Fig. 3(a) and have a domelike shape contained in the underdoped regime with a maximum value at $\delta \approx 0.13$. On the other hand, the amplitudes of electron hopping modulation ($\delta P_{CDW}$) and electron concentration modulation ($\delta n_{CDW}$) are increasing with the decreasing doping, which is in agreement with the measured doping dependence of the CDW critical temperature [4,5]. One should note that the parameter set corresponding to Fig. 3 is close to the one for which good agreement between theory and experiment has been obtained with respect to selected universal properties of the pure superconducting phase in cuprates [39].

As can be seen from Figs. 2 and 3, the $s$-wave ($\delta n_{CDW}$), extended $s$-wave ($\delta P^{s'}_{CDW}$, $\delta\Delta^{s'}_{PDW}$), and $d$-wave ($\delta P^d_{CDW}$, $\delta\Delta^d_{PDW}$) contributions to the pairing and hopping modulations have nonzero values in the obtained CDW+PDW phase. According to the experimental analysis in the large group of copper-based compounds, the dominant $d$-wave form factor is believed to appear. Our calculations show that the $d$-wave form factor amplitudes are significantly larger than the extended $s$-wave correspondents. However, the site-centered $s$-wave contribution to the CDW $\delta n_{CDW}$ is still quite significant within our analysis [see Figs. 2(a) and 2(b), as well as Figs. 3(a) and 3(b)]. Also, we obtain the $\delta\Delta^x_{PDW}$ and $\delta P^x_{CDW}$ form factors, which reflect the inequivalence between the hopping/pairing to the left- and right-hand neighbors of atomic sites (1) and (2). Such a description is necessary in order to obtain the considered periodicity of the hopping and pairing averages.

## IV. OUTLOOK

The present paper concludes our construction of a fairly complete phase diagram for the high-$T_C$ cuprate superconductors as obtained within a single-band model of correlated electrons with the use of the consistent DE-GWF scheme [39–42]. Namely, we have analyzed the coexistence of the pair- and charge-density-wave phases within the Hubbard and $t$-$J$-$U$ models by using the DE-GWF method. The calculations have been carried out for the fixed modulation vector $\mathbf{Q} = (2\pi/3, 0)$, which specifies both the pair- and the charge-density-wave periodicities (as reported in Ref. [22]) and is close to that measured experimentally.

Our results obtained for the $t$-$J$-$U$ model confirm the stability of a pure $d$-wave superconducting phase down to the hole doping $\delta \approx 0.18$, which corresponds to the maximal correlated gap and therefore is identified as the optimal doping. Below that value, a coexistent PDW+CDW phase sets in for which both the $C_4$ and translational symmetries are spontaneously broken. The $d$-wave SC gap parameter is reduced in the PDW+CDW stability regime, and the PDW pairing modulation amplitudes form a domelike shape confined within the underdoped regime. On the other hand, the CDW hopping and electron concentration modulation amplitudes increase with decreasing doping, which is reminiscent of the $T_{CDW}$ doping dependence determined by the x-ray diffraction experiments [4]. Also, the facts that the modulated phase appears in the underdoped regime and that the $d$-wave symmetry modulation form factor is significantly larger than that of the extended $s$ wave agree with the experimental observations. Nevertheless, our approach also leads to a significant contribution of the site-centered CDW ordering, which means that the zero-gap state in the nodal direction is lost.

For the case of the Hubbard model a narrow stability range of the coexistent superconducting-nematic phase appears in between the pure SC and PDW+CDW phases. In the SC+N phase the rotational symmetry is broken; however, the translational symmetry is conserved. Such a phase can be considered a precursor state for the formation of the CDW+PDW phase with decreasing doping. The absence of the SC+N state for the case of the $t$-$J$-$U$ model is due to the negative influence of the exchange term $\sim J$ on the nematic phase stability, which was reported recently [42,46].

Note that in related analysis the intersite Coulomb interaction was included in order to induce the charge-ordered state [34,47–50]. Within that approach the appearance of CDW can be grasped in a straightforward manner. Namely, in the simplest case of a site-centered checkerboard pattern, the role of nonlocal electron repulsion ($\sim V$) is minimal at the cost of the increasing local interaction energy ($\sim U$). In such a case the charge ordering appears after reaching the critical $V$ value [47–50]. For the case of more sophisticated charge orderings, including the bond order, the situation is not so intuitively clear, especially when an additional pair-density-wave modulation comes into play. From our present analysis it follows that the intrasite Coulomb interaction is sufficient to induce both the pure $d$-wave SC and the charge/pair modulated states; hence, the presence of the $V$ term is not required in our approach. However, the stability of the mentioned phases could not be reproduced within our zeroth-order diagrammatic expansion (16), which is equivalent to RMFT. This means that the higher-order terms of the DE-GWF are instrumental for the spontaneous symmetry breaking, here expressed in terms of the formation of SC and PDW/CDW states. The appearance of the bond-ordered state coexisting with $d$-wave SC induced purely by local Coulomb repulsion was also reported recently in Ref. [26], but the results are different from ours.

The principal conclusion from the two models (Hubbard and $t$-$J$-$U$) studied here is that the $t$-$J$-$U$ model provides results which more closely correspond to the experimental data for the CDW+PDW modulated state of the cuprates. In our very recent paper we showed that this model also leads to a good quantitative agreement between theory and experiment for the selected universal characteristics of the pure $d$-wave superconducting state [39]. The parameter set taken in that analysis [39] is close to that taken here. Nevertheless, a proper balance between the symmetry form factors of the CDW+PDW phase is still lacking within the single-band DE-GWF description. The dominant $d$-wave bond-ordered phase, which is believed to appear in many copper-based compounds, can be ascribed to a modulating charge located on the oxygen $2p$ orbitals of the Cu-O plane [9,14]. To incorporate explicitly such a scenario one has to consider a more realistic three-band $d$-$p$ model. However, the application of the DE-GWF method to such a situation introduces a degree of complexity difficult to handle at the present time. We should see progress along this line in the near future, as only then we can reliably estimate the limits of applicability of the one-band effective models.

It should be noted that the appearance of the PDW pattern with the same modulation as that for the CDW phase, as analyzed here, is expected on the symmetry grounds and is in agreement with the Ginzburg-Landau theory. However, it seems reasonable to ask which modulation should be considered as the primary one, CDW or PDW. Within our approach a pure PDW phase (without the charge modulation) has not been found. On the other hand, if we disregard superconductivity in our analysis, a pure CDW pattern (without PDW) appears, and its stability regime is slightly wider than that for the case of the PDW+CDW state. Namely, the upper critical doping for the CDW phase is $\delta \approx 0.2$ for the case of the $t$-$J$-$U$ model instead of $\delta = 0.18$, as it is for the PDW+CDW with the superconducting state included in the calculations. Since the charge modulation can appear without the pairing modulation, we conclude that the CDW phase appears in the underdoped regime as the primary phase, and the modulations of the Cooper-pair condensate are a consequence of the existing charge-density-wave pattern. Nevertheless, the appearance of the pure $d$-wave SC phase pushes the modulated states to lower dopings.

Recently, a more complex interplay between the CDW and PDW orderings has drawn attention [29–31]. Namely, it has been argued that when the PDW state with a modulation vector $\mathbf{Q}_{PDW}$ coexists with uniform $d$-wave superconductivity, it should be related to a two-modulation-vector CDW phase with $\mathbf{Q}^{(1)}_{CDW} = \mathbf{Q}_{PDW}$ and $\mathbf{Q}^{(2)}_{CDW} = 2\mathbf{Q}_{PDW}$. Such a coexistent phase is expected to appear in the situation in which the $d$-wave SC and PDW order parameters are of comparable magnitude. Very recently, it was claimed that such a PDW phase appears in BSCCO in the vortex-core halo induced by the magnetic field, where the pure $d$-wave SC phase is suppressed [28], fulfilling the latter condition. This result is in agreement with the theoretical considerations presented in Ref. [31], which showed that the mentioned type of the PDW/CDW coexistence could appear for substantial magnetic fields (see Fig. 7 of that paper). The two simultaneous periods of the coexistent CDW phase have been measured to be $8a$ and $4a$, which means that the PDW modulation would have a periodicity of $8a$. In order to analyze such a scenario within our approach, one would have to consider modulations with a period of $6a$, which in turn introduces a significant complication to our DE-GWF scheme. Carrying out such an analysis to the higher orders of the diagrammatic expansion is beyond our present computational capabilities. Nevertheless, our theoretical study refers mainly to the experimental verification of PDW with much smaller periodicity ($4a$), which is very close to the CDW pattern periodicity and has been reported in zero magnetic field [22].

## ACKNOWLEDGMENTS

The discussions with M. Fidrysiak and M. Abram are gratefully acknowledged. M.Z. acknowledges financial support from SONATA Grant No. 2016/21/D/ST3/00979 from the National Science Centre (NCN), Poland. J.S. acknowledges financial support from MAESTRO Grant No. DEC-2012/04/A/ST3/00342 from the National Science Centre (NCN) of Poland.

[1] T. Wu, H. Mayaffre, S. Krämer, M. Horvatic, C. Berthier, W. N. Hardy, R. Liang, D. A. Bonn, and M.-H. Julien, Nat. Commun. **6**, 6438 (2015).

[2] A.-J. Achkar, R. Sutarto, X. Mao, F. He, A. Frano, S. Blanco-Canosa, M. Le Tacon, G. Ghiringhelli, L. Braicovich, M. Minola, M. Moretti Sala, C. Mazzoli, R. Liang, D. A. Bonn, W. N. Hardy, B. Keimer, G. A. Sawatzky, and D. G. Hawthorn, Phys. Rev. Lett. **109**, 167001 (2012).

[3] G. Ghiringhelli, M. Le Tacon, M. Minola, S. Blanco-Canosa, C. Mazzoli, N. B. Brookes, G. M. De Luca, A. Frano, D. G. Hawthorn, F. He, T. Loew, M. N. Sala, D. C. Peets, M. Salluzzo, E. Schierle, R. Sutarto, G. A. Sawatzky, E. Weschke, B. Keimer, and L. Braicovich, Science **337**, 821 (2012).

[4] J. Chang, E. Blackburn, A. T. Holmes, N. B. Christensen, J. Larsen, J. Mesot, R. Liang, D. A. Bonn, W. N. Hardy, A. Watenphul, W. von Zimmermann, E. M. Forgan, and S. M. Hayden, Nat. Phys. **8**, 871 (2012).

[5] W. Tabis, Y. Li, M. Le Tacon, L. Braicovich, A. Kreyssig, M. Minola, G. Dellea, E. Weschke, M. J. Veit, M. Ramazanoglu, A. I. Goldman, T. Schmitt, G. Ghiringhelli, N. Barisić, M. K. Chan, C. J. Dorow, G. Yu, X. Zhao, B. Keimer, and M. Graven, Nat. Commun. **5**, 5875 (2014).

[6] E. Blackburn, J. Chang, M. Hücker, A. T. Holmes, N. B. Christensen, R. Liang, D. A. Bonn, W. N. Hardy, U. Rütt, O. Gutowski, M. von Zimmermann, E. M. Forgan, and S. M Hayden, Phys. Rev. Lett. **110**, 137004 (2013).

[7] R. Comin, A. Frano, M. M. Yee, Y. Yoshida, H. Eisaki, E. Schierle, E. Weschke, R. Sutarto, F. He, A. Soumyanarayanan, Y. He, M. Le Tacon, I. S. Elfimov, J. E. Hoffman, and G. A. Sawatzky, B. Keimer, and A. Damascelli, Science **343**, 390 (2014).

[8] E. H. da Silva Neto, P. Aynajian, A. Frano, R. Comin, E. Schierle, E. Weschke, A. Gyenis, J. Wen, J. Schneeloch, Z. Xu, S. Ono, G. Gu, M. Le Tacon, and A. Yazdani, Science **343**, 393 (2014).

[9] R. Comin, R. Sutarto, E. H. da Silva Neto, L. Chauviere, R. Liang, W. N. Hardy, D. A. Bonn, F. He, G. A. Sawatzky, and A. Damascelli, Science **347**, 1335 (2015).

[10] J. M. Tranquada, B. J. Sternlieb, J. D. Axe, Y. Nakamura, and S. Uchida, Nature (London) **375**, 561 (1995).

[11] J. Fink, V. Soltwisch, J. Geck, E. Schierle, E. Weschke, and B. Büchner, Phys. Rev. B **83**, 092503 (2011).

[12] M. Hücker, M. von Zimmermann, Z. J. Xu, J. S. Wen, G. D. Gu, and J. M. Tranquada, Phys. Rev. B **87**, 014501 (2013).

[13] S. Blanco-Canosa, A. Frano, E. Schierle, J. Porras, T. Loew, M. Minola, M. Bluschke, E. Weschke, B. Keimer, and M. Le Tacon, Phys. Rev. B **90**, 054513 (2014).

[14] A. J. Achkar, F. He, R. Sutarto, C. McMahon, M. Zwiebler, M. Hücker, G. D. Gu, R. Ruixing, D. A. Bonn, W. N. Hardy, J. Geck, and D. G. Hawthorn, Nat. Mater. **15**, 616 (2016).

[15] M. Hücker, N. B. Christensen, A. T. Holmes, E. Blackburn, E. M. Forgan, R. Liang, D. A. Bonn, W. N. Hardy, O. Gutowski, M. vom Zimmermann, S. M. Hayden, and J. Chang, Phys. Rev. B **90**, 054514 (2014).

[16] T. Wu, H. Mayaffre, S. Krámer, M. Horvatić, C. Berthier, W. N. Hardy, R. Liang, D. A. Bonn, and M.-H. Julien, Nature (London) **477**, 191 (2011).

[17] M. D. Croitoru, M. Houzet, and A. I. Buzdin, Phys. Rev. Lett. **108**, 207005 (2012).

[18] F. Wu, G. C. Guo, W. Zhang, and W. Yi, Phys. Rev. Lett. **110**, 110401 (2013).

[19] M. D. Croitoru and A. I. Buzdin, Phys. Rev. B **89**, 224506 (2014).

[20] A. Ptok, Eur. Phys. J. B **87**, 2 (2014).

[21] P. Wójcik, M. Zegrodnik, and J. Spałek, Phys. Rev. B **91**, 224511 (2015).

[22] M. H. Hamidian, S. D. Edkins, S. H. Joo, A. Kostin, H. Eisaki, S. Uchida, M. J. Lawler, E.-A. Kin, A. P. Mackenzie, K. Fujita, J. Lee, and J. C. S. Davis, Nature (London) **532**, 343 (2016).

[23] E. Berg, E. Fradkin, and S. A. Kivelson, Nat. Phys. **5**, 830 (2009).

[24] D. F. Agterberg and H. Tsunetsugu, Nat. Phys. **4**, 639 (2008).

[25] Y. Wang, D. F. Agterberg, and A. Chubukov, Phys. Rev. Lett. **114**, 197001 (2015).

[26] J. P. L. Faye and D. Sénéchal, Phys. Rev. B **95**, 115127 (2017).

[27] H. Freire, V. S. de Carvalho, and C. Pépin, Phys. Rev. B **92**, 045132 (2015).

[28] S. D. Edkins *et al.*, arxiv:1802.04673.

[29] D. F. Agterberg and J. Garaud, Phys. Rev. B **91**, 104512 (2015).

[30] Z. Dai, Y.-H. Zhang, T. Senthil, and P. A. Lee, Phys. Rev. B **97**, 174511 (2018).

[31] Y. Wang, S. D. Edkins, M. H. Hamidian, J. C. S. Davis, E. Fradkin, and S. A. Kivelson, Phys. Rev. B **97**, 174510 (2018).

[32] P. Lee, Phys. Rev. X **4**, 031017 (2014).

[33] E. Berg, E. Fradkin, S. A. Kivelson, and J. M. Tranquada, New J. Phys. **11**, 115004 (2009).

[34] A. Allais, J. Bauer, and S. Sachdev, Phys. Rev. B **90**, 155114 (2014).

[35] D. Chowdhury and S. Sachdev, Phys. Rev. B **90**, 245136 (2014).

[36] Y. Wang and A. Chubukov, Phys. Rev. B **90**, 035149 (2014).

[37] H. Meier, C. Pépin, M. Einenkel, and K. B. Efetov, Phys. Rev. B **89**, 195115 (2014).

[38] Y. Wang and A. V. Chubukov, Phys. Rev. B **92**, 245140 (2015).

[39] J. Spałek, M. Zegrodnik, and J. Kaczmarczyk, Phys. Rev. B **95**, 024506 (2017).

[40] M. Zegrodnik and J. Spałek, Phys. Rev. B **95**, 024507 (2017).

[41] M. Zegrodnik and J. Spałek, Phys. Rev. B **96**, 054511 (2017).

[42] M. Zegrodnik and J. Spałek, New J. Phys. **20**, 063015 (2018).

[43] F. Gebhard, Phys. Rev. B **41**, 9452 (1990).

[44] J. Bünemann, T. Schickling, and F. Gebhard, Europhys. Lett. **98**, 27006 (2012).

[45] J. Kaczmarczyk, J. Bünemann, and J. Spałek, New J. Phys. **16**, 073018 (2014).

[46] J. Kaczmarczyk, T. Schickling, and J. Bünemann, Phys. Rev. B **94**, 085152 (2016).

[47] M. Abram, M. Zegrodnik, and J. Spałek, J. Phys.: Condens Matter **29**, 365602 (2017).

[48] A. Amaricci, A. Camjayi, K. Haule, G. Kotliar, D. Tanasković, and V. Dobrosavljević, Phys. Rev. B **82**, 155102 (2010).

[49] H. Terletska, T. Chen, and E. Gull, Phys. Rev. B **95**, 115149 (2017).

[50] K. J. Kapcia, S. Robaszkiewicz, M. Capone, and A. Amaricci, Phys. Rev. B **95**, 125112 (2017).